

## Supplementary Information

### Involvement of Werner syndrome protein in MUTYH-mediated repair of oxidative DNA damage

Radhakrishnan Kanagaraj, Prasanna Parasuraman, Boris Mihaljevic, Barbara van Loon, Kamila Burdova, Christiane König, Antonia Furrer, Vilhelm A. Bohr, Ulrich Hübscher and Pavel Janscak

## Supplementary Materials and Methods

### DNA substrates and siRNA

Oligonucleotides used for gap-filling and primer extension assays were purchased from Purimix and purified by denaturing PAGE. The sequences are:

72-mer template:

3'-ATGTTGGTTCTCGTATGCTGCCGGTCACGGCTTAAGTGT**X**GCGGCCGCG

GGTTGGAGGGCTTATAGATTATG-5'; the bold letter X denotes G or 8-oxo-G. The underlined sequences correspond to the primer-annealing site.

39-mer primer:

5'-TACAACCAAGAGCATACGACGGCCAGTGCCGAATTCACA-3'

32-mer oligonucleotide:

5'-CGCCGGCGCCCAACCTCCCGAATATCTAATAC-3'

The 39-mer primer was 5'-end labeled with T4 polynucleotide kinase (NEB) and  $\gamma$ [<sup>32</sup>P]ATP (GE Healthcare) mixed with appropriate template oligonucleotide at 1:1 (M/M) ratio in the presence of 20 mM Tris-HCl (pH 7.4) and 150 mM NaCl, heated at 95°C for 10 minutes and then slowly cooled down to room temperature. To generate gapped substrates, annealing mixtures also contained the equimolar amount of the 32-mer oligonucleotide phosphorylated at the 5'-end by T4 polynucleotide kinase (NEB) prior to annealing.

A 5'-end biotinylated version of the above 39-mer oligonucleotide was purchased from MWG-Biotech AG.

All siRNA oligoduplexes used in this study were purchased from Microsynth. The sequences of the sense strands of these duplexes are shown below:

siWRN: 5'-UAGAGGGAAACUUGGCAAAdTdT-3'

siPol $\lambda$ : 5'-CAAAAGUACUUGCAAAGAUAdTdT-3'

siMUTYH: 5'-UCACAUCAAGCUGACAUCAAGUAAdTdT-3'

siCtrl: 5'-CGUACGCGGAUACUUCGAdTdT-3'

### Antibodies

Affinity purified rabbit polyclonal antibodies against human Pol $\lambda$  (used for immunofluorescence staining at a 1:500 dilution) and WRN (used for immunofluorescence staining at a 1:500 dilution) were described previously (1,2). Rabbit polyclonal antibody against human Pol $\lambda$  used for immunoblotting was purchased from Bethyl Laboratories (IHC-00325). Rabbit polyclonal antibody against mouse Pol $\lambda$  was a kind gift from Dr. L. Blanco. Rabbit polyclonal antibody against human WRN used for

immunoprecipitation was purchased from Abcam (ab17988). Goat polyclonal antibody against human WRN used for immunoblotting was purchased from Santa Cruz (sc-1956). Mouse monoclonal anti-WRN antibodies were purchased from BD Biosciences (611169; used for immunoblotting) and Abcam (ab 66601; used for immunofluorescence staining at a 1:50 dilution). Mouse monoclonal antibodies against MUTYH and 8-oxo-G were purchased from Abcam (ab55551) and Millipore (MAB3560, clone 483.15), respectively. Antibodies against TFIIH (rabbit polyclonal),  $\beta$ -tubulin (mouse monoclonal) and cyclin-A (mouse monoclonal) were from Santa Cruz.

## **Cell lines**

Immortalized Pol $\lambda^{+/+}$  and Pol $\lambda^{-/-}$  mouse embryonic fibroblasts (MEFs) were obtained from Dr. S.H. Wilson (3). Pol $\lambda^{-/-}$  MEFs stably transduced with a retroviral vector encoding human Pol $\lambda$ -myc were described previously (4). SV-40 immortalized WS fibroblasts (AG11395) stably expressing WRN-E84A and WRN-K577M, respectively, were maintained as previously described (5).

## **BrdU incorporation analysis**

BrdU was added to media to a final concentration 10  $\mu$ M at 30 minutes before harvesting the cells. Staining with FITC-conjugated anti-BrdU antibody was done according to manufacturer protocol (BD Biosciences). Flow cytometry analysis was performed using FACSCalibur (BD Biosciences) and FlowJo software.

## **GST pull-down assay**

Binding of Pol $\lambda$  to GST-tagged fragments of WRN was tested as previously described (2). Briefly, bacterially expressed GST-WRN fusion proteins were bound to glutathione-Sepharose beads (20  $\mu$ l; GE Healthcare) and incubated with 0.5  $\mu$ g of recombinant human Pol $\lambda$  for 2 hours at 4°C. Bound proteins were analyzed by Western blotting. Glutathione beads coated with GST-protein only were used as control.

## **Annexin V-binding assay**

Cell death was monitored using Annexin V-Cy3 apoptosis detection kit (APOAC; Sigma) according to the manufacturer's instructions. Briefly, cells were either left untreated or treated with 500  $\mu$ M H<sub>2</sub>O<sub>2</sub> for 2 hours, and subsequently released into fresh DMEM medium. After 48 hours, cells were harvested and spotted on a glass slide. Live and dead cells were detected by labeling with 6-carboxyfluorescein (green fluorescence) and Annexin V (red fluorescence), respectively. Cells were immediately observed by fluorescence microscope. The percentage of dead cells was calculated relative to total number of cells and plotted using GraphPad Prism as mean  $\pm$  SD. Data from at least two independent experiments were plotted.

### MUTYH-initiated repair assay

5'-labeled 100-mer DNA duplex containing a 8-oxo-G:A mispair was prepared as previously described (1). Reaction mixtures (10  $\mu$ l) contained 50 mM Tris-HCl (pH 7.5), 20 mM KCl, 2 mM DTT and 5  $\mu$ M dNTPs. Concentrations of MUTYH, APE1 and Pol $\lambda$  were 50, 0.6 and 2 nM, respectively. WRN was present at concentrations ranging from 0 to 32 nM as indicated. Reaction mixtures containing MUTYH and DNA substrate were treated as follows: (i) incubation for 5 minutes at 30°C, (ii) addition of APE1 and 0.5 mM Mg<sup>2+</sup>, (iii) incubation for 10 minutes at 30°C, (iv) addition of dNTPs, WRN and Pol $\lambda$ , (v) incubation 15 minutes at 37°C. All reactions were stopped by addition of standard denaturing gel loading buffer (95% formamide, 10 mM EDTA, xylene cyanol and bromophenol blue), heated at 95°C for 3 minutes and loaded on a 7M urea/15% polyacrylamide gel. Gels were scanned using Typhoon 9400 phosphorimager and quantified using ImageQuant software.

### Biotin pull-down assay

Gapped DNA duplexes containing the biotinylated version of the 39-mer oligonucleotide were prepared as described above. Before annealing, the 32-mer oligonucleotide was phosphorylated at the 5'-end using T4 polynucleotide kinase (NEB). Binding reactions (50  $\mu$ l) were carried out at 37 °C for 5 minutes in a buffer containing 50 mM Tris-HCl (pH 7.0), 0.25 mg/ml BSA, 1 mM DTT, 1 mM MgCl<sub>2</sub> and 1  $\mu$ M dCTP. Pol $\lambda$  and WRN were present at a concentration of 20 nM and DNA substrates (with or without 8-oxo-G lesion) at a concentration of 100 nM. DNA-protein complexes were isolated using Streptavidin agarose beads (20  $\mu$ l; Invitrogen). After incubation on ice for 10 minutes, beads were washed thrice with PBS and bound proteins were analyzed by Western blotting using antibodies against WRN and Pol $\lambda$ .

### Supplementary References

1. van Loon,B. and Hubscher,U. (2009) An 8-oxo-guanine repair pathway coordinated by MUTYH glycosylase and DNA polymerase lambda. *Proc. Natl. Acad. Sci. USA*, **106**, 18201-18206.
2. Saydam,N., Kanagaraj,R., Dietschy,T., Garcia,P.L., Pena-Diaz,J., Shevelev,I., Stagljar,I. and Janscak,P. (2007) Physical and functional interactions between Werner syndrome helicase and mismatch-repair initiation factors. *Nucleic Acids Res.*, **35**, 5706-5716.
3. Braithwaite,E.K., Prasad,R., Shock,D.D., Hou,E.W., Beard,W.A. and Wilson,S.H. (2005) DNA polymerase lambda mediates a back-up base excision repair activity in extracts of mouse embryonic fibroblasts. *J. Biol. Chem.*, **280**, 18469-18475.
4. Wimmer,U., Ferrari,E., Hunziker,P. and Hubscher,U. (2008) Control of DNA polymerase lambda stability by phosphorylation and ubiquitination during the cell cycle. *EMBO Rep.*, **9**, 1027-1033.
5. Pirzio, L.M., Pichierri, P., Bignami, M. and Franchitto, A. (2008) Werner syndrome helicase activity is essential in maintaining fragile site stability. *J Cell Biol*, **180**, 305-314.

**Supplementary Table 1.** Quantitative analysis of immunofluorescence images of U2OS cells stained for WRN and Pol $\lambda$  prior to and after H<sub>2</sub>O<sub>2</sub> treatment

	Nuclei scored as foci positive <sup>a</sup> (%)			Nuclei with co-localizing foci <sup>b</sup> (%)
	WRN	Pol $\lambda$	WRN and Pol $\lambda$	
Untreated	6	7.5	4.5	4
H <sub>2</sub> O <sub>2</sub>	45	65	41	34.5

Representative images are shown in Figure 3A.

At least 300 nuclei from three independent experiments were analyzed.

<sup>a</sup>Foci positive nuclei: if nuclei contained at least ten distinct foci.

<sup>b</sup>Co-localization positive nuclei: if  $\geq 75\%$  of WRN foci overlapped with Pol $\lambda$  foci.

**Supplementary Table 2.** Quantitative analysis of immunofluorescence images of U2OS cells stained for WRN and 8-oxo-G prior to and after H<sub>2</sub>O<sub>2</sub> treatment

	Nuclei scored as foci positive <sup>a</sup> (%)			Nuclei with co-localizing foci <sup>b</sup> (%)
	WRN	8-oxo-G	WRN and 8-oxo-G	
Untreated	4	3	3	2
H <sub>2</sub> O <sub>2</sub>	47.4	51	45.5	42

Representative images are shown in Figure 4A (*first two rows*).

At least 300 nuclei from three independent experiments were analyzed.

<sup>a</sup>Foci positive nuclei: if nuclei contained at least six distinct foci.

<sup>b</sup>Co-localization positive nuclei: if  $\geq 75\%$  of 8-oxo-G foci overlapped with WRN foci.

**Supplementary Table 3.** Quantitative analysis of immunofluorescence images of U2OS cells stained for Pol $\lambda$  and 8-oxo-G prior to and after H<sub>2</sub>O<sub>2</sub> treatment

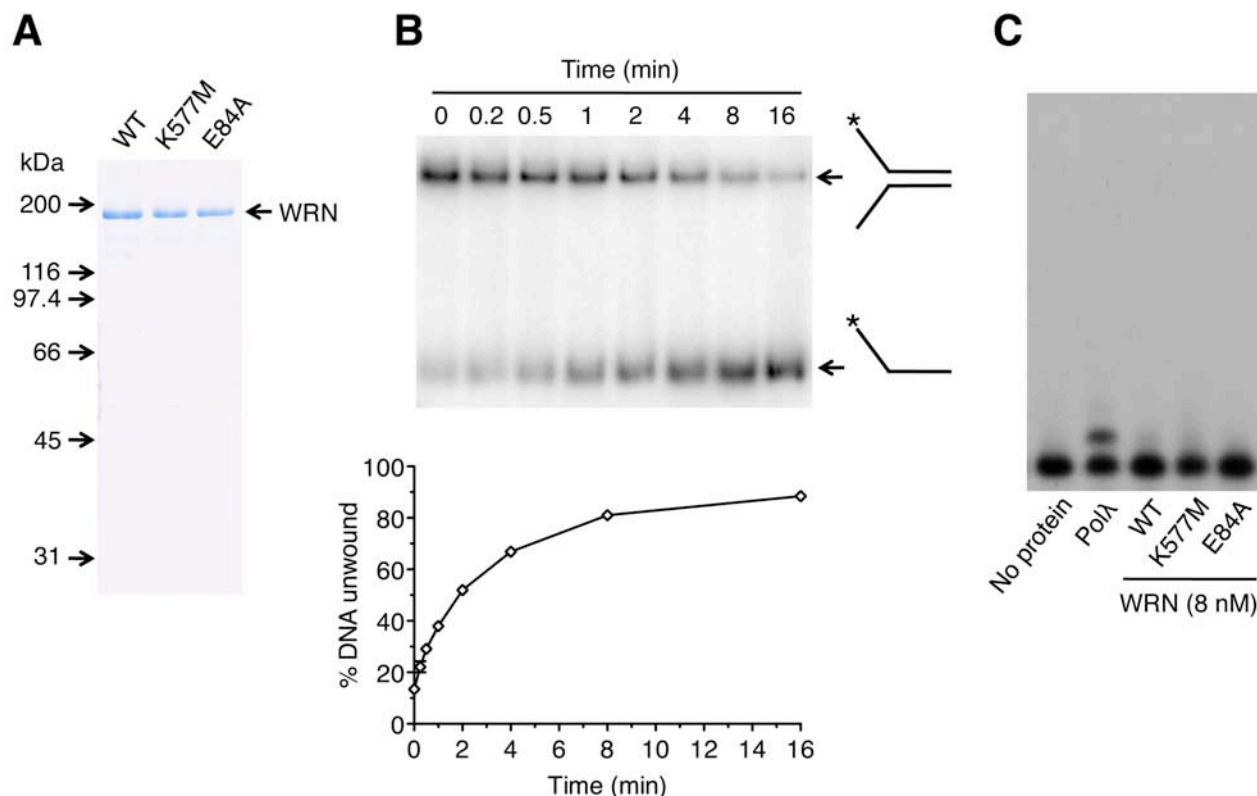
	Nuclei scored as foci positive <sup>a</sup> (%)			Nuclei with co-localizing foci <sup>b</sup> (%)
	Pol $\lambda$	8-oxo-G	Pol $\lambda$ and 8-oxo-G	
Untreated	5.5	4	2	2
H <sub>2</sub> O <sub>2</sub>	61.5	54	52.5	50.5

Representative images are shown in Figure 4A (*last two rows*).

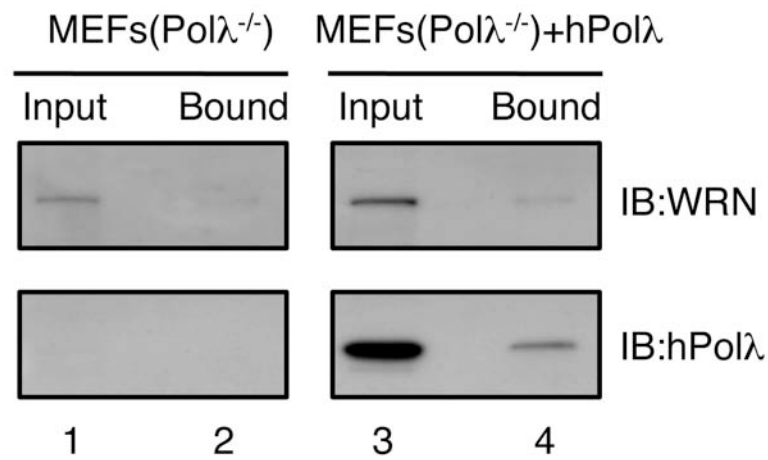
At least 300 nuclei from three independent experiments were analyzed.

<sup>a</sup>Foci positive nuclei: if nuclei contained at least six distinct foci.

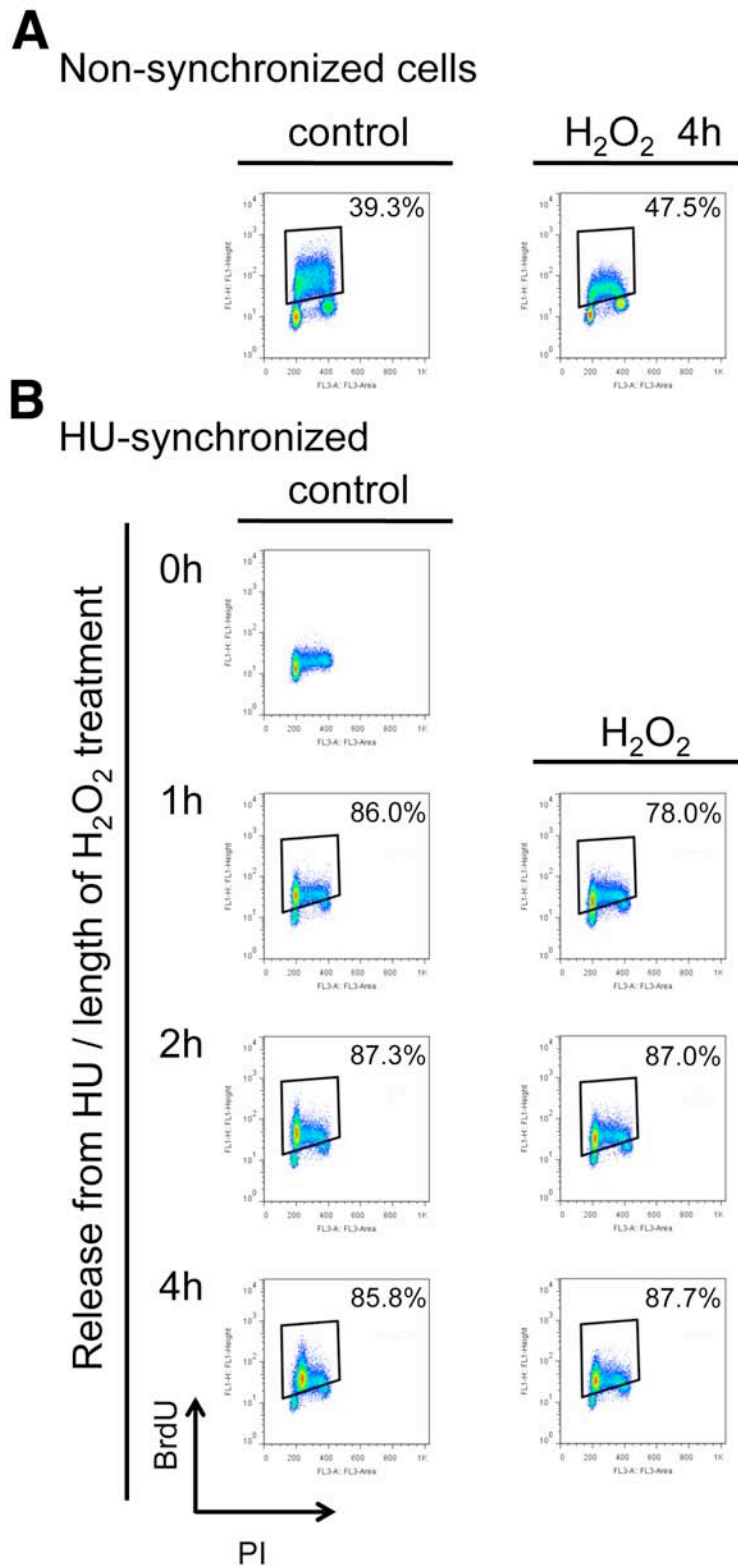
<sup>b</sup>Co-localization positive nuclei: if  $\geq 75\%$  of 8-oxo-G foci overlapped with Pol $\lambda$  foci.



**Figure S1.** Characterization of purified wild-type and mutant forms of WRN protein used in this study. (A) SDS PAGE analysis. Gel was stained with Coomassie Brilliant Blue R-250. The molecular masses of protein standards are indicated on the left. (B) Kinetics of WRN-mediated unwinding of 30-bp forked DNA duplex. Reaction contained 1 nM [ $^{32}$ P]DNA. (*Top panel*) Reaction aliquots at indicated time points were analyzed by native PAGE followed by phosphorimaging. Schemes of the substrate and the reaction products are also shown. The position of the radioactive label (5'-end) is indicated by asterisks. (*Bottom panel*) Gel image was quantified using ImageQuant software. Relative concentration of unwound products calculated as a percentage of total DNA is plotted. (C) Preparations of WRN and its mutants do not contain a contaminating DNA polymerase activity. The primer extension assay was carried out as described in Experimental Procedures using the lesion-free template. WRN and its mutants were present at a concentration of 8 nM and Pol $\lambda$  at a concentration of 6 nM.

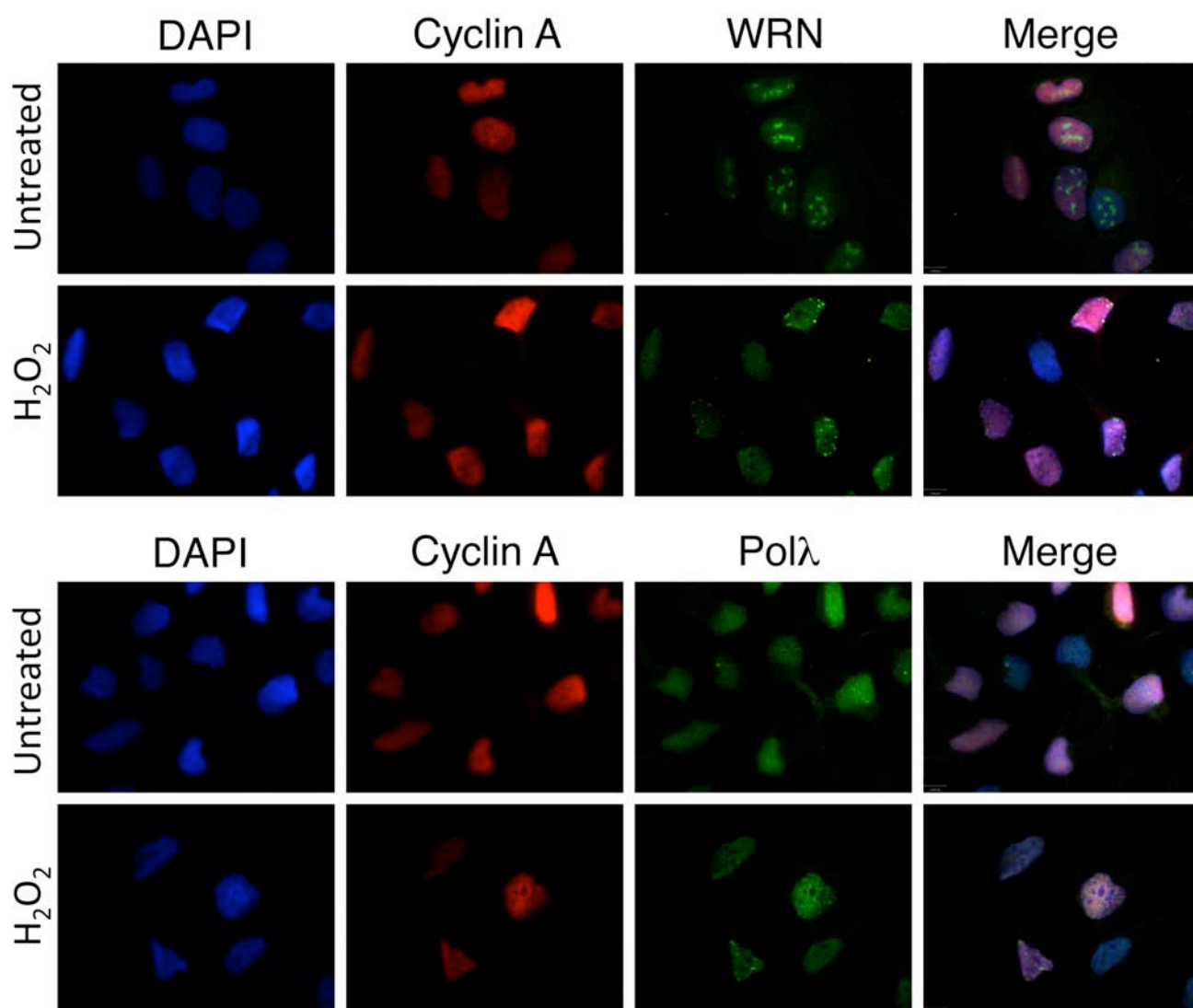


**Figure S2.** Protein recruitment assay using biotinylated 8-oxo-G:A hairpin substrate and whole cell extract from Pol $\lambda^{-/-}$  MEFs (*left panel*) or Pol $\lambda^{-/-}$  MEFs complemented with human Pol $\lambda$  (hPol $\lambda$ ) cDNA (*right panel*). Pol $\lambda^{-/-}$  MEFs were stably transduced with a retroviral vector expressing Myc-tagged hPol $\lambda$ . Cell extracts were incubated with the DNA substrate for 8 minutes before formaldehyde crosslinking. Bound proteins were analyzed by western blotting. Blots were probed with antibodies against WRN and Pol $\lambda$ . 10% of input material was loaded.

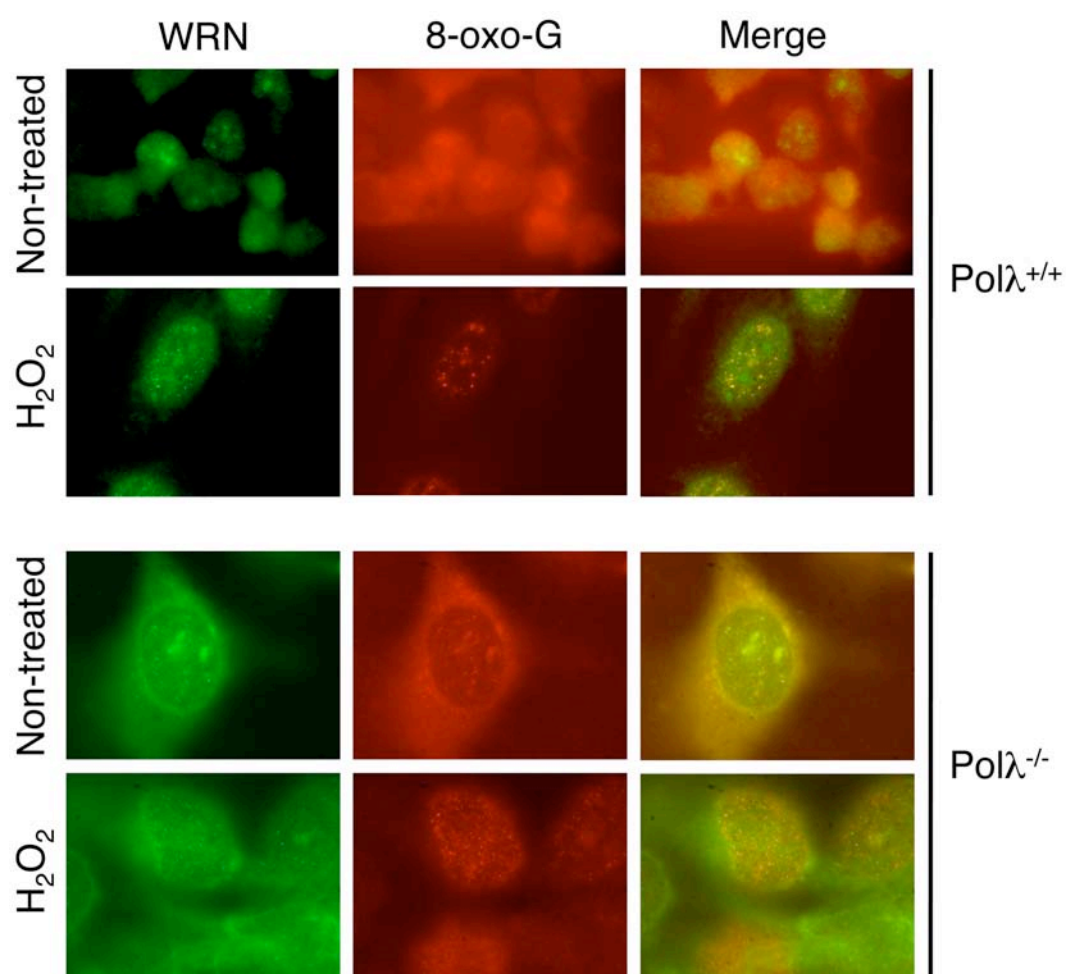


**Figure S3.** Flow cytometry analysis of BrdU incorporation in asynchronous U2OS cells (A) and hydroxyurea (HU)-synchronized U2OS cells (B) prior to and after treatment with hydrogen peroxide (500  $\mu$ M). BrdU incorporation (FITC) (y axis) was measured against DNA content (propidium iodide, PI) (x axis). BrdU was added 30 minutes before harvesting the cells. The percentage of cell incorporating BrdU is indicated.

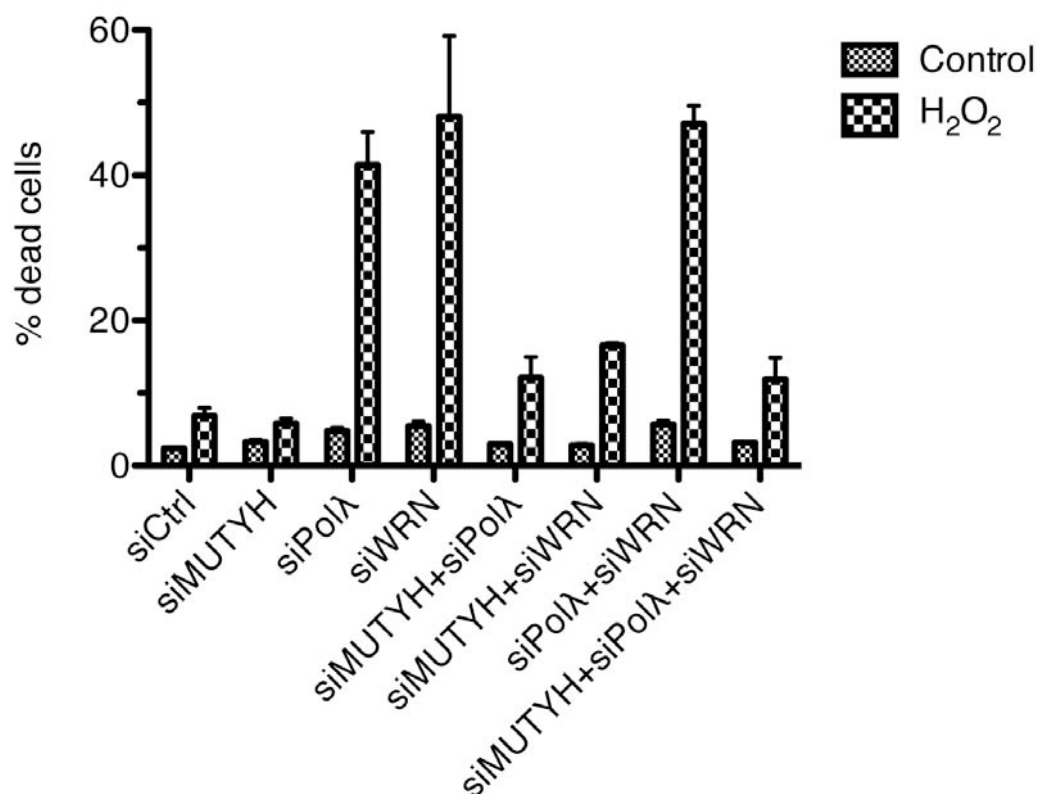




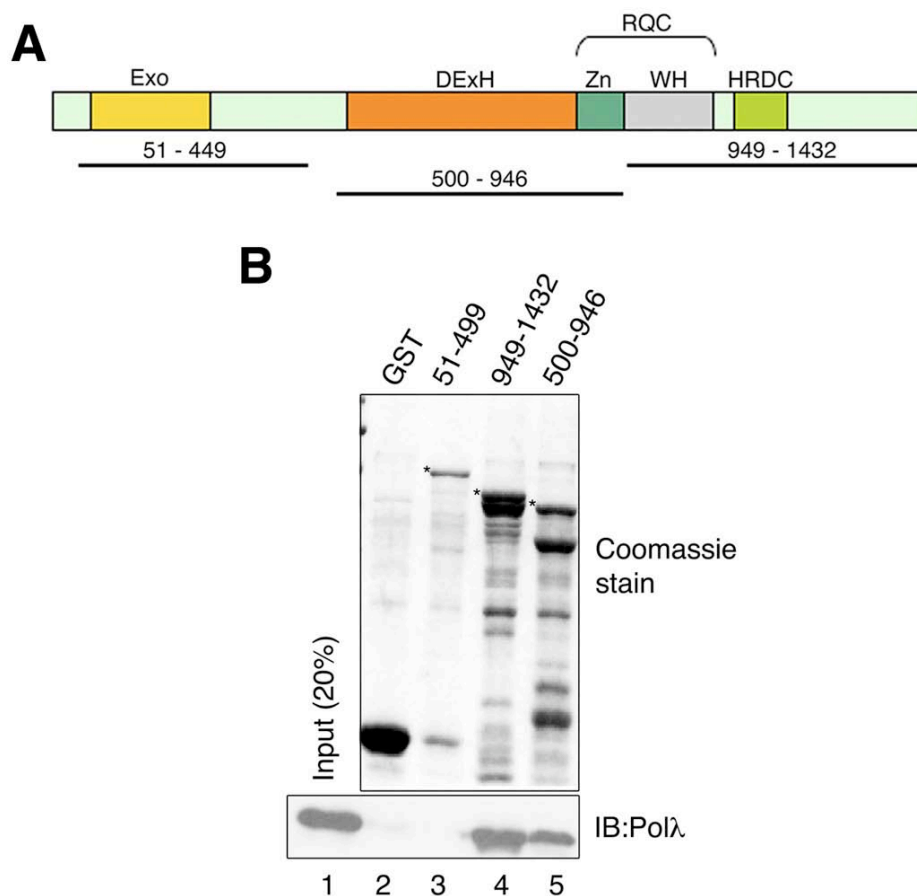
**Figure S4.** S/G2 phase-specific formation of WRN and Polλ foci in response to oxidative stress. Cells grown on glass coverslips were either left untreated or treated with 500  $\mu$ M  $H_2O_2$  for 2 hours. After treatment, cells were fixed and immunostained using antibodies against WRN (green) and cyclin A (red) (*top panel*) or against Polλ (green) and cyclin A (red) (*bottom panel*). DAPI staining of the nucleus is shown in blue. Cells positive for cyclin A (dispersed nuclear staining) are in S/G2, whereas cells lacking cyclin A are in G1.



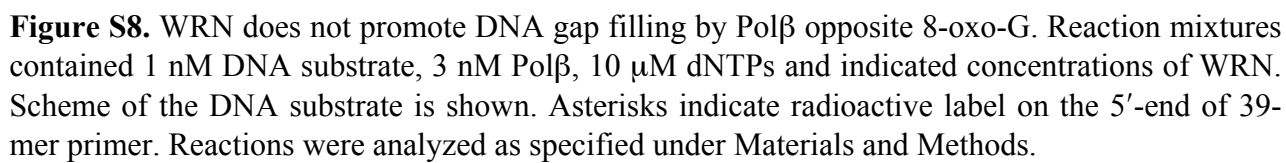
**Figure S5.** Polλ is required for the recruitment of WRN to sites of 8-oxo-G lesions. Polλ<sup>+/+</sup> (*top panel*) and Polλ<sup>-/-</sup> (*bottom panel*) mouse embryonic fibroblasts were treated with 100 μM H<sub>2</sub>O<sub>2</sub> (or left untreated) for 2 hours. Cells were fixed and immunostained to visualize WRN (green) and 8-oxo-G (red). Representative images are shown.



**Figure S6.** Depletion of MUTYH suppresses cell death caused by WRN- or Polλ-deficiency under conditions of oxidative stress. HeLa cells transfected with indicated siRNAs were treated with 500  $\mu$ M H<sub>2</sub>O<sub>2</sub> for 2 hours or mock-treated. 48 hours post-treatment, percentage of dead cells was determined using Annexin V-binding assay as described in Supplementary Materials and Methods. The data points represent the mean of two independent experiments with at least 1000 cells scored in each experiment. siCtrl, siMUTYH, siWRN and siPolλ represent siRNA against luciferase, MUTYH, WRN and Polλ, respectively.



**Figure S7.** Mapping of Polλ-interacting domain of WRN. (A) Domain organization of WRN. Exo, Exonuclease domain; DExH, helicase domain conserved in the DExH family of helicases; RQC, RecQ C-terminal domain composed of Zn-binding (Zn) and winged-helix (WH) subdomains; HRDC, helicase and RNase D C-terminal domain. The black lines indicate WRN fragments used. (B) GST pull-down assay. The indicated WRN fragments were produced as fusions with GST and immobilized on glutathione beads. Binding of purified recombinant Polλ to the beads was analyzed by Western blotting. The Coomassie Brilliant Blue-stained gel from SDS-PAGE analysis of the GST-WRN fragments isolated on glutathione beads is also shown. Asterisks indicate the GST-WRN fragments. The additional protein bands correspond to proteolytic degradation products as determined by immunoblotting using an anti-GST antibody (data not shown). Lane 1, 20% of input of Polλ. IB, immunoblotting.



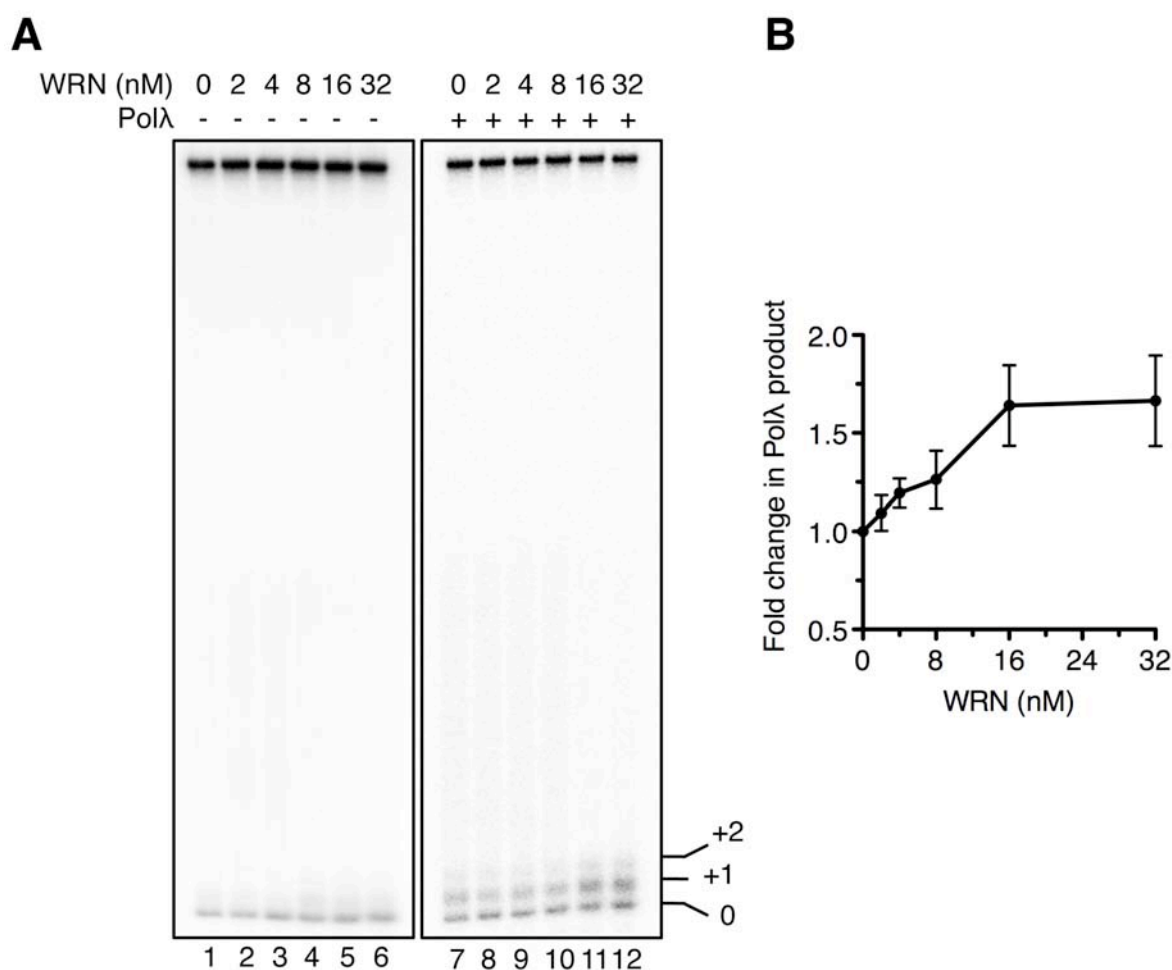


**Figure S9.** WRN promotes MUTYH/Polλ-mediated repair of 8-oxo-G:A mispairs. (A, *left panel*) Effect of WRN on the removal of A mispaired to 8-oxo-G mediated by MUTYH and APE1. Reaction mixtures contained 1 nM DNA substrate, 50 nM MUTYH, 0.6 nM APE1, 5μM dNTPs and indicated concentrations of WRN. Reactions were analyzed as specified under Supplemental Experimental Procedures. (A, *right panel*) Effect of WRN on Polλ-mediated bypass of 8-oxo-G following the removal of mispaired A by MUTYH and APE1. Reaction mixtures contain 1 nM DNA substrate, 50 nM MUTYH, 0.6 nM APE1, 2 nM Polλ and 5μM dNTPs. Reactions were analyzed as in (A). The positions of MUTYH/APE1 cleavage product (0) and Polλ extension products (+1, +2) are indicated. (B) Quantification of Polλ activity in the presence of MUTYH, APE1 and increasing amounts of WRN from three different experiments as the one documented in (A); error bars,  $\pm$  SD values.

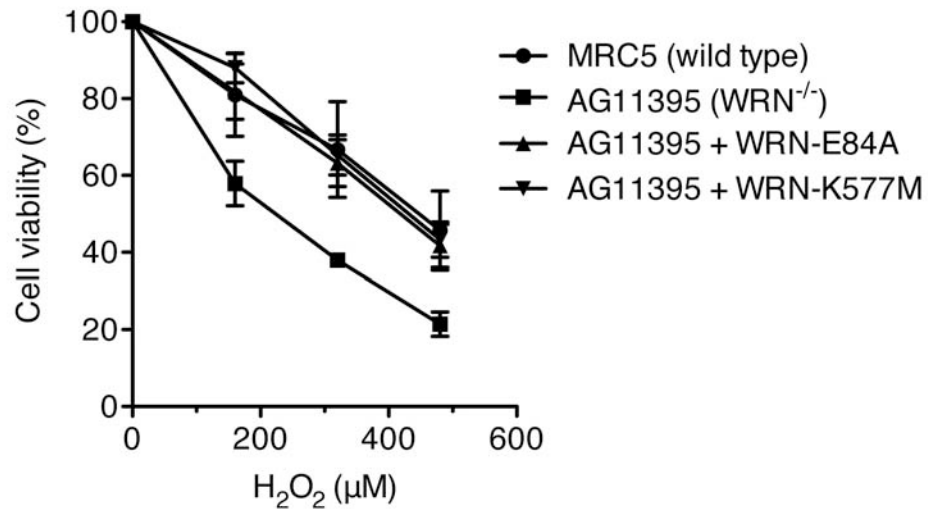


**Figure S10.** Catalytically inactive mutants of WRN restore tolerance to oxidative stress in Werner syndrome cells. Indicated cell lines were treated with different concentrations of H<sub>2</sub>O<sub>2</sub> for 2 hours. Cell viability assay was performed as described in Materials and Methods. Data points represent the mean of three independent experiments  $\pm$  SD. WRN-E84A, exonuclease-dead mutant of WRN; WRN-K577M, helicase-dead mutant of WRN.

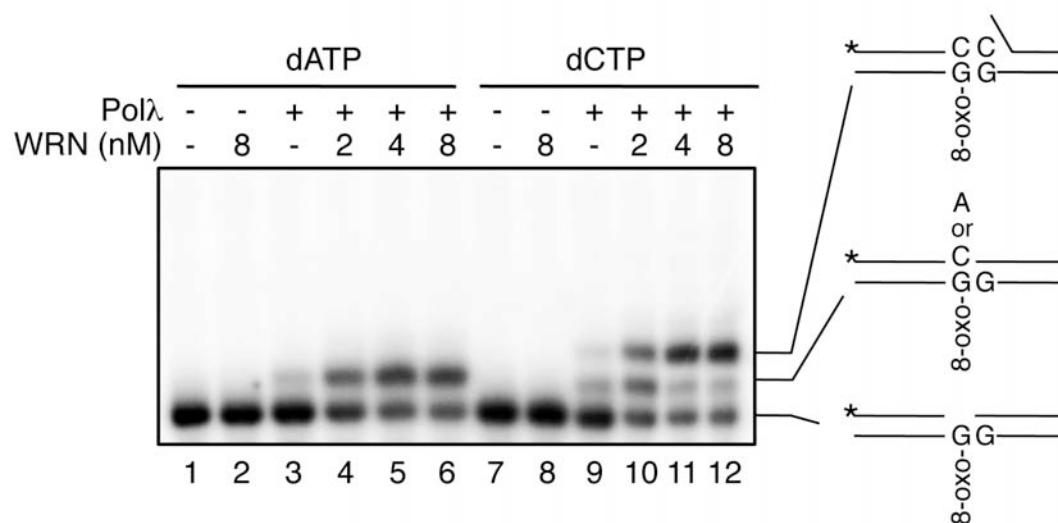


**Figure S11.** Effect of WRN on bypass of 8-oxo-G by Polλ on gapped DNA duplex as measured by single nucleotide incorporation assay. Reactions were carried out in the presence of either 10 μM dATP or 10 μM dCTP as described under Materials and methods and as documented in Figure 7A.



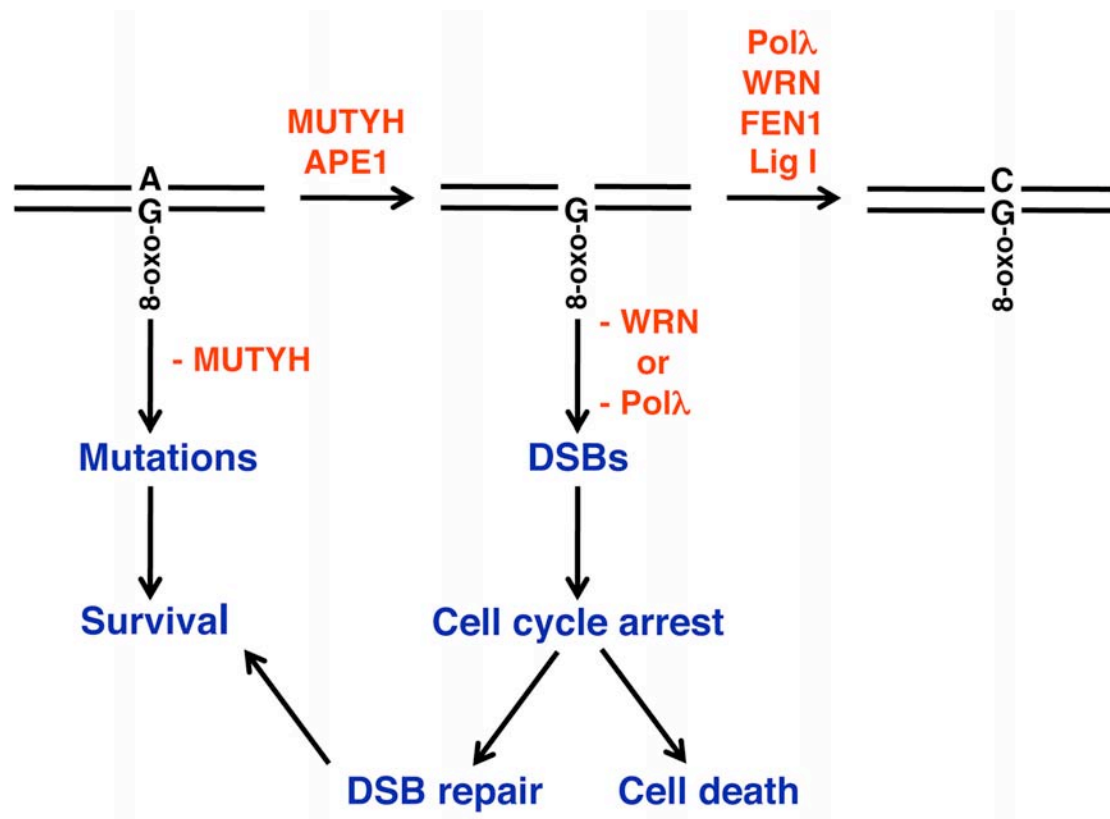


**Figure S12.** MUTYH-initiated repair of 8-oxo-G:A mismatch. WRN promotes 8-oxo-G bypass by DNA polymerase  $\lambda$  (Pol $\lambda$ ). Proposed phenotypic consequences of defects in different steps of repair of 8-oxo-G:A mismatches are also shown. Mutations (G:C to T:A transversions) or DNA double-strand breaks (DSBs) are generated during the next round of DNA replication.